

# Multidentate Tetrahydrofurfuryloxy Ligand in a Ziegler–Natta Catalyst Studied by Molecular Modeling

Zygmunt Flisak

*Institute of Chemistry, University of Opole, Oleska 48, 45-052 Opole, Poland*

*Received June 10, 2008; Revised Manuscript Received August 12, 2008*

**ABSTRACT:** The transition from a generation III Ziegler–Natta catalyst with a monodentate Lewis base to a more modern generation IV/V system, containing a tetrahydrofuran derivative, the tetrahydrofurfuryloxy  $\text{C}_4\text{H}_7\text{O}-\text{CH}_2\text{O}^-$  bidentate ligand (THFFO), was studied by means of molecular modeling and DFT calculations. This particular ligand was carefully chosen so that it remained in the titanium coordination sphere in the model active site. With such a constraint, the dual role of tetrahydrofurfuryloxy was identified: it was demonstrated how the presence of this ligand limits the number of isomeric active sites as well as enhances the selectivity of the species that can still exist. The results indicate that the catalyst with a bidentate ligand attains good selectivities, albeit at a cost of activity.

## 1. Introduction

The classical Ziegler–Natta catalysts, invented over a half-century ago, have been modified extensively to improve their activity and selectivity. These efforts led to the consecutive generations of such systems. As a result of all the modifications, the modern industrially applied catalysts, classified as generation IV and V, contain multidentate Lewis bases (usually diesters or diethers).<sup>1,2</sup> Polypropylene of well-defined properties can be obtained over such systems with relatively high yield.

Although the first theoretical papers on the coordinative olefin polymerization appeared over 30 years ago and dealt almost exclusively with ethylene, it was only within the past decade that the researchers attempted the quantitative explanation of the role of electron donors in the heterogeneous systems and their influence on selectivities. Shiga carried out the analysis of propylene polymerization over titanium and zirconium catalysts using the PIO method;<sup>3</sup> one of the systems discussed in his work contained a Lewis base. Bhaduri et al.<sup>4</sup> compared different catalysts bearing alkoxy ligands in the process of ethylene and propylene polymerization. Their study however, neither took the support into account nor predicted any changes in the selectivities of these catalysts. Toto et al.<sup>5</sup> studied the coordination of 1,3-diethers on the surface of the support by means of molecular mechanics and semiempirical methods. Although they succeeded in determining the preferential modes of coordination with respect to numerous factors (such as different lateral cuts of the support, the electron donor structure and its conformation), their study addressed the problem of regio- and stereoselectivity indirectly due to omission of polymerization active sites. Very recently, the group of Cavallo<sup>6</sup> extended these findings and reported the results of the DFT calculations on the first model of active sites composed of the support, titanium atom, growing polymer chain and, most of all, a bidentate donor attached to the surface of magnesium chloride. Stereoselectivity of their model was unambiguous and demonstrated in an elegant way; nevertheless, the regioselectivity was still negligible. On the contrary, the calculations conducted in the Ziegler group<sup>7</sup> indicated that a monodentate Lewis base attached to the titanium atom in a model active site is sufficient to create a regioselective and stereoselective catalyst.

In this setting, it is worth examining whether a bidentate ligand attached directly to the titanium atom improves the selectivities of the catalyst. Theoretical calculations<sup>6,8</sup> suggest that a typical bidentate ligand (e.g., diethyl phthalate) binds to the surface of the support much stronger than to the titanium

tetrachloride molecule, but both processes are thermodynamically favored. Therefore, introducing a ligand with two donor atoms of comparable basicity (as in the case of 1,3-diethers) implies the necessity of considering a large number of potential active sites, since the ligand can coordinate to the titanium and magnesium atoms according to various scenarios, i.e., binding only to the support as described in ref 6, bridging both the Ti and Mg atoms, or attaching exclusively to the former. To overcome this problem, a special kind of bidentate ligand, having two oxygen atoms of extremely different coordination number, can be selected. The 2-tetrahydrofurfuryloxy (see Figure 1), despite its limited industrial importance, fulfills this criterion. If it is applied as an internal Lewis base in the form of the titanium complex, one can guarantee that the strong  $\text{Ti}-\text{O}_{\text{alkoxide}}$  bond never gets broken, as demonstrated by the experimental and theoretical works.<sup>9,10</sup> At the same time, the ligand's ability to coordinate to the support is still retained. Such an approach in electron donor selection makes it possible to isolate the interactions of the ligand with the transition metal atom from the interactions with the support.

## 2. Computational Details

The computational procedures applied were similar to these described in refs 7 and 11–13 with several minor modifications. The ONIOM method<sup>14</sup> implemented in the Gaussian 03 package<sup>15</sup> was applied to divide the models of active sites into two layers. The *high* layer was treated with the density functional of Tao, Perdew, Staroverov, and Scuseria (TPSS),<sup>16</sup> whose performance in the field of transition metal compounds was reported to be superior<sup>17</sup> to the widely used B3LYP functional,<sup>18,19</sup> whereas the UFF molecular mechanics<sup>20</sup> was used in the *low* layer. The 6-31G(d) basis set<sup>21</sup> was applied to the C, H, and O atoms and the LANL2DZ double- $\zeta$  basis set with the effective core potential<sup>22–25</sup> to the Ti atom.

The transition states were located by scanning the potential energy surface along the reaction coordinate, which was the distance between the carbon atoms of the bond to be formed as

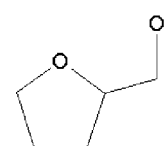


**Figure 1.** Tetrahydrofurfuryloxy ligand.

**Table 1.** Diastereomers Possible for the [Mabcdef] Octahedral Complex

	L	M	N
1	ab	ab	ab
	cd	ce	cf
	ef	df	de
2	ac	ac	ac
	bd	be	bf
	ef	df	de
3	ad	ad	ad
	bc	be	bf
	ef	cf	ce
4	ae	ae	ae
	bc	bd	bf
	df	cf	cd
5	af	af	af
	bc	bd	be
	de	ce	cd

a result of insertion. The step of the linear transit procedure was 0.1 Å; in certain cases it was decreased to 0.05 Å.

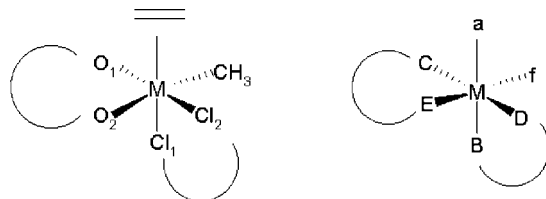
### 3. Results and Discussion

**3.1. Design and Construction of Active Sites.** The models of the active sites were constructed according to the procedure described and thoroughly validated elsewhere.<sup>7,11–13</sup> The current analysis was restricted to the (110) lateral cut of MgCl<sub>2</sub> with the four-coordinated magnesium atoms exposed, since it was demonstrated theoretically that the model catalyst based on it exhibits not only greater stability, but also higher activity comparing with other lateral cuts of catalytic importance.<sup>7,11,26</sup> This assumption is further rationalized by the latest experimental and theoretical findings,<sup>27</sup> indicating that the surface of the ball-milled magnesium chloride does contain ca. 20% of the four-coordinated magnesium species, corresponding probably to (110) cuts.

The molecule of the tetrahydrofurfuryloxy ligand (see Figure 1) has two oxygen atoms of markedly different donor numbers. These O atoms can potentially coordinate either to the Mg atoms of the support or the Ti atom of the catalytic site, or both. The ligand can be absorbed on the surface of the support only in the chelating mode<sup>6</sup> due to short O–O interatomic distance. A dinuclear complex of titanium tetrachloride and tetrahydrofurfuryloxy, in which two chlorine atoms form a bridge between the titanium atoms, has been successfully synthesized and characterized.<sup>9</sup> The DFT calculations in the gas phase, carried out within the current work, show that the dimer easily dissociates—the energy required for this process does not exceed 10 kcal/mol and the entropic contribution further diminishes the positive Gibbs free energy of dissociation. Therefore, the monomeric form was considered in further calculations.

Using this introductory information, it is now imperative to analyze the number of possible isomers (diastereomers and enantiomers) of the catalytic species. This analysis can be conveniently carried out using the scheme developed by Bailar,<sup>28</sup> which is claimed to be the most successful method of isomer enumeration.<sup>29</sup> In this method, the ligands located trans to each other are listed in pairs in a table containing all possible diastereomers of the octahedral complex with six different ligands, [Mabcdef]; see Table 1. For other complexes, suitable changes are made to this table, e.g., multidentate ligands are denoted with capital letters and certain diastereomers are subsequently eliminated. For the full explanation of the procedure, see the original references.

The active site discussed in this work, together with a coordinated olefin molecule, can be approximated as an octahedral titanium complex with multidentate ligands and assigned with the [Ma(BD)(CE)f] formula; see Figure 2. In this

**Figure 2.** Octahedral active site.**Table 2.** Ten Possible Diastereomers for the [Ma(BD)(CE)f] Octahedral Complex: Each of Them Has an Enantiomeric Form

	L	M	N
1	aB	—	aB
	CD	—	Cf
	Ef	—	DE
2	—	aC	aC
	—	BE	Bf
	—	Df	DE
3	aD	aD	—
	BC	BE	—
	Ef	Cf	—
4	aE	—	aE
	BC	—	Bf
	Df	—	CD
5	af	—	af
	BC	—	BE
	DE	—	CD

notation, M refers to the titanium atom, (CE) represents the tetrahydrofurfuryloxy ligand with two oxygen atoms of a different donor number (O<sub>alkoxide</sub> and O<sub>ether</sub>, respectively), (BD) corresponds to the surface of the support with two chlorine atoms of different donor number (actually, one of the Cl atoms, marked as D, originates from the precursor, which does not affect the reasoning below); finally a and f stand for two separate monodentate ligands: the olefin and the growing polymer chain, respectively. For the [Mabcdef] complex, there are 15 possible diastereomers and each of these diastereomers has an enantiomeric form, thus doubling the number of structures to be considered. Such a conclusion might discourage from any attempt of modeling olefin polymerization over the catalyst derived from such a complex, as the number of possible active sites,  $\pi$ -complexes, and transition states seems untreatable within a reasonable amount of time, even employing state-of-the-art computing facilities.

The existence of any multidentate ligand in an octahedral complex simplifies this picture. For example, it is obvious that a bidentate ligand cannot span trans positions; therefore, certain configurations listed in Table 1 are not allowed. Following the Bailar scheme for our case, the M1, N3, and M5 elements should be eliminated, because the O<sub>ether</sub> and the O<sub>alkoxide</sub> atoms, denoted as E and C, respectively, cannot occupy the trans positions; therefore, they cannot appear next to each other in any cell of the table. The elements L2 and M4 are also removed to prevent the violation of the same rule by the support. This approach reduces the number of isomers to 20—see Table 2.

Fortunately, this number is further minimized due to the nature of the constituents of the catalytic system and the chemistry of the polymerization process. It can be calculated taking into account certain restrictions that fall beyond the assumptions of the regular Bailar method, but are still well treated by it. For example, the mechanism of coordinative olefin polymerization<sup>30</sup> assumes the existence of the transition state, in which the olefin and the alkyl group attached to the titanium atom form the four-membered ring; therefore the (a and f) species are allowed to occupy only cis positions—this is equivalent to the cis requirement for a bidentate ligand, described above. Thus, the number of isomers drops to 16 by elimination of the L5 and N5 elements. This result is consistent with the

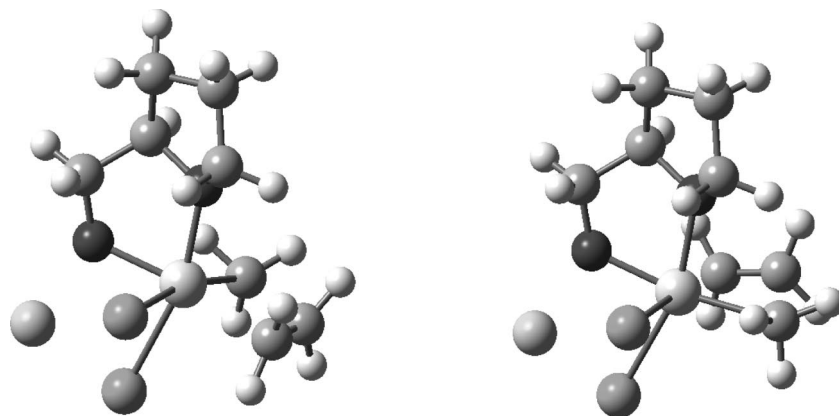


**Figure 3.** Two diastereomers, M2 and M3, of possible ethylene insertion transition states. For the sake of clarity, the support is omitted from this figure, except for one magnesium (and one chlorine) atom located in the lower part of the picture.

calculation carried out by means of the FORTRAN code published in ref 31. Furthermore, the flat surface of the (110) lateral cut imposes even more constraints on the structure of the model active site—it should be mentioned that the bulky tetrahydrofurfuryloxy ring cannot be aligned parallelly to the support surface with both oxygen atoms bound to the titanium atom, which means that C and E cannot occupy the equatorial positions, while B stays at the axial position. This eliminates five cells: L1, N1, N2, L3, and N4 (all the elements discarded from Table 2 are printed in *italics*). Furthermore, the alkoxide oxygen atom, together with the chlorine atom form the anchor between the transition metal complex and the support. For steric reasons discussed above, this role cannot be played by the ether oxygen atom—there would be a strong repulsion between the support surface and the heterocyclic ring. This condition requires that B and E should occupy exclusively *trans* positions, which is fulfilled only by M2 and M3 (printed in **boldface** in Table 2). Both of them have  $\Delta$  and  $\Lambda$  enantiomers, which presumably exhibit complementary preference toward *re* and *si* enantiofaces of propylene.

To conclude this section, it should be stated that for ethylene, there are only two diastereomers of transition states (Figure 3) that have to be treated separately in the following DFT analysis. They differ only in the arrangement of the alkyl group (which is a model of the growing polymer chain and the olefin). The M2 diastereomer has the olefin *trans* to the O<sub>alkoxide</sub> atom, whereas in M3, the methyl group occupies this position. Since propylene is a prochiral monomer, calculations for this olefin extend to four possible transition states within one diastereomer; they correspond to two modes of insertion and two enantiofaces of propylene.

**3.2. Catalytic Activity in Ethylene and Propylene Polymerization.** The first part of the computational assessment of the catalytic active sites with the multidentate tetrahydrofurfuryloxy ligand focuses on the activity toward ethylene and propylene. For the purpose of comparison, the insertion barriers for the catalyst with no Lewis base as well as the system modified by tetrahydrofuran are recalculated using the method described in the Computational Details section above, but not all the barriers for the generic catalyst without Lewis base are calculated. Although such systems, especially the generic one, have been studied extensively over the decades, no reports on using the TPSS functional on them have been published yet.

It should be noted that the processes of the olefin uptake calculated within this work turned out to be exoenergetic in many cases. To avoid reporting low or even negative barriers (especially in the case of the active sites with no Lewis base), the internal insertion barriers, calculated with respect to the  $\pi$ -complex rather than the isolated active site and the olefin,

**Table 3.** Internal Barriers of Ethylene and Propylene Insertion (kcal/mol)

	no Lewis base	THF	THFFO (M2)	THFFO (M3)
Initiation				
$\Delta E_{\text{ins}}^{\#}$ , ethylene	7.6	6.9	15.7	11.7
$\Delta E_{\text{ins}}^{\#}$ , propylene max	—	7.9	17.8	12.4
$\Delta E_{\text{ins}}^{\#}$ , propylene min	—	5.8	14.4	11.3
Propagation				
$\Delta E_{\text{ins}}^{\#}$ , ethylene	—	5.1	13.9	9.8
$\Delta E_{\text{ins}}^{\#}$ , propylene max	—	7.6	15.3	9.1
$\Delta E_{\text{ins}}^{\#}$ , propylene min	—	2.0	12.6	7.8

are given in Table 3. For propylene, there is a range of insertion barriers due to the fact that the uptake energies depend on the orientation of the olefin molecule. The maximum internal insertion barrier was calculated as the energy difference between the lowest-lying transition state and the  $\pi$ -complex of the most exoenergetic formation. On the contrary, the  $\pi$ -complex of the least exoenergetic (or sometimes most endoenergetic) formation was chosen for the calculation of the minimum internal insertion barrier. The minimum propylene insertion barriers calculated in this way are slightly lower than the corresponding ethylene barriers, which would suggest unexpected results contradictory to the experimental works. However, it should be stressed that the entropic contribution (not calculated within this work) would make all the Gibbs free energies of  $\pi$ -complex formation positive; thus, the external insertion barrier (calculated with respect to isolated active site and the olefin) becomes a better determinant of the catalytic activity. Apart from that, the  $\pi$ -complexes exist in equilibrium; they can decompose, form again, or even isomerize by the rotation of the olefin in the plane of the double bond with a low energetic barrier of the process.<sup>32</sup>

The internal insertion barriers of the first and subsequent olefin molecules into the Ti—C bond (initiation and propagation) indicate that the introduction of a multidentate ligand impairs the catalytic activity toward ethylene and propylene—see Table 3. For ethylene, there is no pronounced difference in activity when tetrahydrofuran is introduced into the titanium coordination sphere, comparing with the catalyst with no Lewis base; on the contrary, the presence of tetrahydrofurfuryloxy markedly increases the barriers of insertion. The propagation barriers are lower than those of initiation, independently of the kind of olefin and the active site. Finally, the active site marked THFFO(M2) is significantly less active than its isomer for both monomers.

**3.3. Regio- and Stereoselectivity.** To analyze the regio- and stereoselectivity of the generation IV/V catalyst, the relative barriers for the two modes of insertion (1,2- and 2,1-), as well



**Table 4. Relative Barriers of Propylene Insertion (in kcal/mol)**

	THF	THFFO (M2)	THFFO (M3)
Initiation			
1,2 re	0.6	0.0	0.4
1,2 si	0.0	0.6	0.0
2,1 re	3.6	1.8	3.8
2,1 si	6.5	1.9	3.6
Propagation			
1,2 re	3.2	0.0	0.0
1,2 si	0.0	4.3	2.3
2,1 re	2.3	2.2	3.4
2,1 si	5.7	1.5	3.7

**Table 5. Regio- and Stereoselectivity**

	THF	THFFO (M2)	THFFO (M3)
Initiation			
$\Delta\Delta E_{\text{regio}}$	3.6	1.8	3.8
$\Delta\Delta E_{\text{stereo}}$	0.6	0.6	0.4
Propagation			
$\Delta\Delta E_{\text{regio}}$	2.3	2.2	3.4
$\Delta\Delta E_{\text{stereo}}$	3.2	4.3	2.3

as two enantiofaces of propylene (re and si), have been compared against the catalyst with a monodentate Lewis base. There are insertion barriers corresponding to both initiation (where the growing polymer chain is represented by the methyl group) and propagation (where previous 1,2-insertion resulted in the isobutyl group attached to the titanium atom) listed in Table 4. It is obvious that the choice of the barrier reported (internal or external) has no effect on the conclusions related to selectivities, since the relative rather than absolute heights of the barriers are compared. Therefore, the following convention was applied in Table 4: for each model of the active site and kind of the process (initiation and propagation), the lowest propylene insertion barrier serves as a reference (the value of 0.0) and the other barriers are reported with respect to this value.

Using this data, it is possible to assess the preference for the particular mode of insertion and propylene enantioface by calculating  $\Delta\Delta E_{\text{regio}}$  and  $\Delta\Delta E_{\text{stereo}}$  according to the following algorithm. First, the barriers are sorted in the ascending order. For all the cases analyzed within this work, the lowest insertion barrier corresponds always to 1,2-insertion (with either re or si enantioface of the olefin, depending on the configuration of the site). Then, the difference between the two lowest barriers is calculated and reported as  $\Delta\Delta E_{\text{regio}}$  if the second barrier corresponds to 2,1-insertion and  $\Delta\Delta E_{\text{stereo}}$  if the second barrier is related to the other propylene enantioface within the 1,2- mode of insertion. Finally, the difference between the first and the third insertion barrier is calculated in the same way to find the missing value of  $\Delta\Delta E_{\text{regio}}$  or  $\Delta\Delta E_{\text{stereo}}$ , respectively. The results of this procedure, listed in Table 5, indicate that at the initiation stage, all the active sites are regioselective, but not stereoselective, which is in line with both experimental<sup>33,34</sup> and computational<sup>35–38</sup> findings, reported in the literature for a variety of heterogeneous and homogeneous systems. The THFFO(M2) site is less regioselective, comparing not only with the THFFO(M3) species but also with the site modified by a monodentate base. In the propagation step, a moderate drop in regioselectivity (except for the THFFO(M2) site) and a significant boost in stereoselectivity occur simultaneously. Now all the sites turn out to be both regioselective and stereoselective. The catalyst with tetrahydrofurfuryloxide seems to outperform the system with tetrahydrofuran in terms of selectivities. However, it is not known (and difficult to decide) whether this improvement compensates the significantly lower activity of the catalyst modified by a bidentate base—see Table 3 and discussion in the previous subsection.

#### 4. Concluding Remarks

Careful choice of a Lewis base (which, unlike widely used phthalates and diesters, has limited commercial application) made it possible to isolate the influence of a bidentate ligand coordinated directly to the transition metal atom on the activity and selectivity of the heterogeneous  $\text{MgCl}_2$ -supported coordinative olefin polymerization catalyst. The increase in both regio- and stereoselectivity, comparing with the systems of earlier generations, can be attributed to two separate factors.

1. Elimination of one isomer of the potential active sites. There are only two diastereomers possible, each with an enantiomeric form. In the case of a monodentate base, one more species of erratic catalytic properties may form (although with a low probability; this was discussed in ref 7).

2. Adjusting the properties of the existing active sites by controlling their electronic properties and steric hindrance around the transition metal atom.

In this respect, the bidentate ligand coordinated to the transition metal atom resembles diethers analyzed recently in the Cavallo group,<sup>6</sup> where both factors were also present: the ligands eliminated nonstereoselective cuts of the support and existed in the vicinity of the active site, thus affecting its catalytic properties.

Bearing in mind these similarities, it is reasonable to anticipate that DFT calculations on a model catalyst with a multidentate ligand coordinated both to the support and the transition metal atom would produce promising results in terms of even higher selectivities.

**Acknowledgment.** The author thanks Krzysztof Szczegot and Marek Wasielewski (University of Opole) for thought-provoking discussions. Wrocław Supercomputing and Networking Centre as well as Academic Computer Centre CYFRONET AGH (Grant No. MNiSW/SGI3700/UOpolski/126/2006) are acknowledged for generous allotment of computer time. This work was partially supported by the Polish Ministry of Science and Higher Education (grant No. N205 267835).

**Supporting Information Available:** Cartesian coordinates of optimized propylene insertion transition states for the M2 and M3 isomers of model active sites. This material is available free of charge via the Internet at <http://pubs.acs.org>.

#### References and Notes

- Galli, P.; Vecellio, G. *Prog. Polym. Sci.* **2001**, *26*, 1287.
- Moore, E. P., Jr., Ed.; *Polypropylene Handbook*; Karl Hanser Verlag: Munich, 1996 p 11.
- Shiga, A. *Res. Chem. Intermed.* **2002**, *28*, 485.
- Bhaduri, S.; Mukhopadhyay, S.; Kulkarni, S. A. *J. Organomet. Chem.* **2003**, *671*, 101.
- Toto, M.; Morini, G.; Guerra, G.; Corradini, P.; Cavallo, L. *Macromolecules* **2000**, *33*, 1134.
- Correa, A.; Piemontesi, F.; Morini, G.; Cavallo, L. *Macromolecules* **2007**, *40*, 9181.
- Flisak, Z.; Ziegler, T. *Macromolecules* **2005**, *38*, 9865.
- Cavallo, L.; Piero, S. D.; Ducéré, J.-M.; Fedele, R.; Morini, G.; Piemontesi, F.; Tolazzi, M. *J. Phys. Chem. C* **2007**, *111*, 4412.
- Sobota, P.; Utiko, J.; Szafert, S.; Szczegot, K. *J. Chem. Soc., Dalton Trans.* **1997**, 679.
- Flisak, Z.; Szczegot, K. *J. Mol. Catal. A* **2003**, *206*, 429.
- Seth, M.; Margl, P. M.; Ziegler, T. *Macromolecules* **2002**, *35*, 7815.
- Seth, M.; Ziegler, T. *Macromolecules* **2003**, *36*, 6613.
- Seth, M.; Ziegler, T. *Macromolecules* **2004**, *37*, 9191.
- Maseras, F.; Morokuma, K. *J. Comput. Chem.* **1995**, *16*, 1170.
- Frisch, M. J.; Trucks, G. W.; Schlegel, H. B.; Scuseria, G. E.; Robb, M. A.; Cheeseman, J. R.; Montgomery, Jr., J. A.; Vreven, T.; Kudin, K. N.; Burant, J. C.; Millam, J. M.; Iyengar, S. S.; Tomasi, J.; Barone, V.; Mennucci, B.; Cossi, M.; Scalmani, G.; Rega, N.; Petersson, G. A.; Nakatsuji, H.; Hada, M.; Ehara, M.; Toyota, K.; Fukuda, R.; Hasegawa, J.; Ishida, M.; Nakajima, T.; Honda, Y.; Kitao, O.; Nakai, H.; Klene, M.; Li, X.; Knox, J. E.; Hratchian, H. P.; Cross, J. B.; Bakken, V.; Adamo, C.; Jaramillo, J.; Gomperts, R.; Stratmann, R. E.; Yazyev,

- O.; Austin, A. J.; Cammi, R.; Pomelli, C.; Ochterski, J. W.; Ayala, P. Y.; Morokuma, K.; Voth, G. A.; Salvador, P.; Dannenberg, J. J.; Zakrzewski, V. G.; Dapprich, S.; Daniels, A. D.; Strain, M. C.; Farkas, O.; Malick, D. K.; Rabuck, A. D. V.; Raghavachari, K.; Foresman, J. B.; Ortiz, J. V.; Cui, Q.; Baboul, A. G.; Clifford, S.; Cioslowski, J.; Stefanov, B. B.; Liu, G.; Liashenko, A.; Piskorz, P.; Komaromi, I.; Martin, R. L.; Fox, D. J.; Keith, T.; Al-Laham, M. A.; Peng, C. Y.; Nanayakkara, A.; Challacombe, M.; Gill, P. M. W.; Johnson, B.; Chen, W.; Wong, M. W.; Gonzalez, C.; Pople, J. A. *Gaussian 03, Revision C.02*; Gaussian, Inc.: Wallingford, CT, 2004.
- (16) Tao, J. M.; Perdew, J. P.; Staroverov, V. N.; Scuseria, G. *Phys. Rev. Lett.* **2003**, *91*, 146401.
- (17) Furche, F.; Perdew, J. P. *J. Chem. Phys.* **2006**, *124*, 044103.
- (18) Becke, A. D. *J. Chem. Phys.* **1993**, *98*, 5648.
- (19) Lee, C.; Yang, W.; Parr, R. G. *Phys. Rev. B* **1988**, *37*, 785.
- (20) Rappe, A. K.; Casewit, C. J.; Colwell, K. S.; Goddard III, W. A.; Skiff, W. M. *J. Am. Chem. Soc.* **1992**, *114*, 10024.
- (21) Ditchfield, R.; Hehre, W. J.; Pople, J. A. *J. Chem. Phys.* **1971**, *54*, 724.
- (22) Dunning Jr., T. H.; Hay, P. J. *Modern Theoretical Chemistry*; Schaefer, H. F., Ed.; Plenum Press: New York, 1976; Vol. 3, p 1.
- (23) Hay, P. J.; Wadt, W. R. *J. Chem. Phys.* **1985**, *82*, 270.
- (24) Wadt, W. R.; Hay, P. J. *J. Chem. Phys.* **1985**, *82*, 284.
- (25) Hay, P. J.; Wadt, W. R. *J. Chem. Phys.* **1985**, *82*, 299.
- (26) Boero, M.; Parrinello, M.; Weiss, H.; Hüfner, S. *J. Phys. Chem. A* **2001**, *105*, 5096.
- (27) Busico, V.; Causá, M.; Cipullo, R.; Credendino, R.; Cutillo, F.; Friederichs, N.; Lamanna, R.; Segre, A.; Castelli, V. V. A. *J. Phys. Chem. C* **2008**, *112*, 1081.
- (28) Bailar, J. C., Jr. *J. Chem. Educ.* **1957**, *34*, 334.
- (29) Purcell, F. K.; Kotz, J. C. *Inorganic Chemistry*; W. B. Saunders: Philadelphia, 1977.
- (30) Cossee, P. *J. Catal.* **1964**, *3*, 80.
- (31) Bennett, W. E. *Inorg. Chem.* **1969**, *8*, 1325.
- (32) Cavallo, L.; Guerra, G.; Corradini, P. *J. Am. Chem. Soc.* **1998**, *120*, 2428.
- (33) Zambelli, A.; Sacchi, M. C.; Locatelli, P.; Zannoni, G. *Macromolecules* **1982**, *15*, 211.
- (34) Longo, P.; Grassi, A.; Pellicchia, C.; Zambelli, A. *Macromolecules* **1987**, *20*, 1015.
- (35) Corradini, P.; Barone, V.; Guerra, G. *Macromolecules* **1982**, *15*, 1242.
- (36) Cavallo, L.; Guerra, G.; Oliva, L.; Vacatello, M.; Corradini, P. *Polym. Commun.* **1989**, *30*, 16.
- (37) Corradini, P.; Guerra, G.; Cavallo, L. *Acc. Chem. Res.* **2004**, *37*, 231.
- (38) Castonguay, L. A.; Rappé, A. K. *J. Am. Chem. Soc.* **1992**, *114*, 5832.

MA801311V